

8-16-2003

Phase Changes in Internally Mixed Maleic Acid/ Ammonium Sulfate Aerosols

Sarah D. Brooks

University of Colorado, Boulder

Rebecca M. Garland

University of Colorado, Boulder

Matthew E. Wise

University of Colorado, Boulder

Anthony J. Prenni

University of Colorado, Boulder

Melinda Cushing

University of Colorado, Boulder

See next page for additional authors

Follow this and additional works at: <http://commons.cu-portland.edu/msfacultyresearch>

 Part of the [Chemistry Commons](#)

Recommended Citation

Brooks, Sarah D.; Garland, Rebecca M.; Wise, Matthew E.; Prenni, Anthony J.; Cushing, Melinda; Hewitt, Erika; and Tolbert, Margaret A., "Phase Changes in Internally Mixed Maleic Acid/Ammonium Sulfate Aerosols" (2003). *Faculty Research*. 73.
<http://commons.cu-portland.edu/msfacultyresearch/73>

This Article is brought to you for free and open access by the Math & Science Department at CU Commons. It has been accepted for inclusion in Faculty Research by an authorized administrator of CU Commons. For more information, please contact libraryadmin@cu-portland.edu.

Authors

Sarah D. Brooks, Rebecca M. Garland, Matthew E. Wise, Anthony J. Prenni, Melinda Cushing, Erika Hewitt,
and Margaret A. Tolbert

Phase changes in internally mixed maleic acid/ammonium sulfate aerosols

Sarah D. Brooks, Rebecca M. Garland, Matthew E. Wise, Anthony J. Prenni, Melinda Cushing, Erika Hewitt, and Margaret A. Tolbert

Department of Chemistry and Biochemistry and Cooperative Institute for Research in Environmental Sciences, University of Colorado, Boulder, Colorado, USA

Received 22 November 2002; revised 18 February 2003; accepted 2 May 2003; published 15 August 2003.

[1] A temperature controlled flow tube system equipped with Fourier transform infrared (FTIR) detection of particle phase and relative humidity was used to measure the deliquescence and efflorescence of ammonium sulfate, maleic acid, and internally mixed maleic acid/ammonium sulfate particles. Our results indicate that maleic acid aerosols begin to take up water starting at a low relative humidity, $\sim 20\%$, and continue the constant uptake of water until the final deliquescence relative humidity (DRH), 89% , is reached. Internally mixed particles containing maleic acid and ammonium sulfate were found to deliquesce at a lower relative humidity (RH) than either of the pure species. Efflorescence studies indicated that while pure maleic acid particles crystallize at $\sim 18\%$ RH, pure ammonium sulfate and all mixed aerosols effloresce at or just below 30% RH. Taken together, our results suggest that the presence of water-soluble organics internally mixed with ammonium sulfate aerosol could increase the range of conditions under which the aerosol is a solution. **INDEX TERMS:** 0305 Atmospheric Composition and Structure: Aerosols and particles (0345, 4801); 0320 Atmospheric Composition and Structure: Cloud physics and chemistry; 0340 Atmospheric Composition and Structure: Middle atmosphere—composition and chemistry; **KEYWORDS:** deliquescence, efflorescence, aerosol phase changes, maleic acid, organics, FTIR

Citation: Brooks, S. D., R. M. Garland, M. E. Wise, A. J. Prenni, M. Cushing, E. Hewitt, and M. A. Tolbert, Phase changes in internally mixed maleic acid/ammonium sulfate aerosols, *J. Geophys. Res.*, 108(D15), 4487, doi:10.1029/2002JD003204, 2003.

1. Introduction

[2] While it is well known that aerosols can directly and indirectly impact the Earth's climate, there are large uncertainties in quantifying the expected effect. Part of the uncertainty arises because of the varying size, shape, chemical composition, and phase of atmospheric aerosols. In particular, recent radiative transfer calculations show a very strong dependence of the radiative forcing on the phase of ammonium sulfate aerosols at 80% relative humidity (RH) (S. T. Martin, Dependence of radiative forcing on aerosol phase, submitted to *Atmospheric Chemistry and Physics*, 2003). In addition to impacts on climate, aerosol phase can influence the rate of heterogeneous chemical reactions. For example, the hydrolysis of N_2O_5 to form nitric acid depends strongly on liquid water content with reaction probabilities of $0.02\text{--}0.06$ and <0.003 , for liquid and solid ammonium sulfate, respectively [Hu and Abbatt, 1997; Mozurkewich and Calvert, 1988].

[3] While the deliquescence (uptake of water) and efflorescence (loss of water) of pure ammonium sulfate are well established [Onasch et al., 1999], recent field data shows evidence that atmospheric sulfate particles may be composed of 50% or more organic material by mass [Murphy et al., 1998; Saxena and Hildemann, 1996]. At several conti-

mental sites in Europe, 60% of the organic carbon content of the tropospheric aerosol has been identified as water-soluble organics [Krivacsy et al., 2001]. A separate study found that mono- and dicarboxylic acids alone comprised an average of 11% of the total organic carbon measured in cloud water over rural Austria [Loflund et al., 2002]. While insoluble organics may inhibit water uptake by atmospheric aerosols [Andrews and Larson, 1993; Ellison et al., 1999; Tervahattu et al., 2002], water-soluble organics may enhance water uptake or may have little impact [Cruz and Pandis, 2000; Hameri and Rood, 1992]. The effect of adding organic compounds may vary with the specific type of organic as well as the ratio of organic to inorganic in the aerosol.

[4] Attempts to quantitatively model how the presence of water-soluble organics will affect water uptake by aerosols have been hindered by a dearth of laboratory data. Predictions derived from the Gibbs-Duhem equation indicate that the deliquescence relative humidity (DRH) of one electrolyte in the presence of another will always be lower than the DRHs of the single components [Wexler and Seinfeld, 1991]. Clegg et al. [2001] have modeled the deliquescence of a few multicomponent solutions of inorganic electrolytes and organic molecules at 273.15 K. They find that the presence of the organics lowers the deliquescence relative humidity of the inorganics. This trend has recently been confirmed experimentally by our group and others [Brooks et al., 2002; Choi and Chan, 2002b; Cruz and Pandis, 2000].

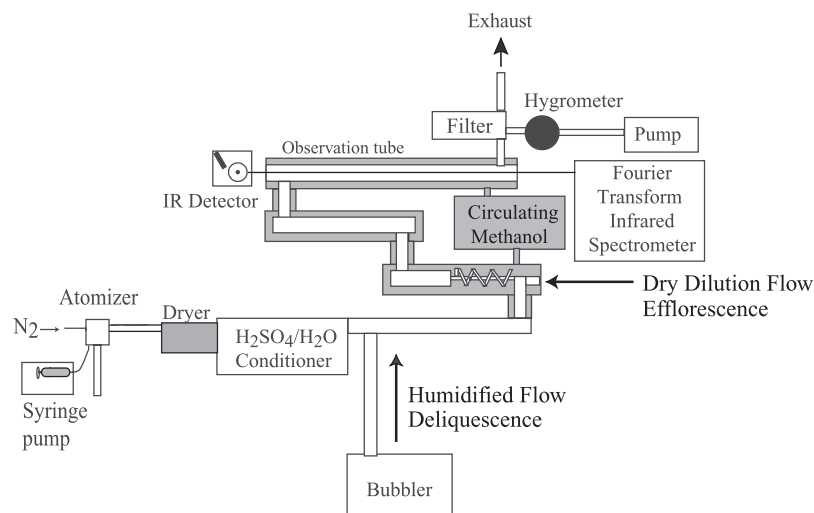


Figure 1. Schematic diagram of the FTIR flow tube system.

[5] In the absence of laboratory measurements, UNIFAC (UNIQUAC Functional Group Activity Coefficients) predictions are often used in modeling studies. A recent combined measurement and modeling effort by *Peng et al.* [2001] shows that water activity predictions for dicarboxylic acids generally agreed with measured water activity within 40% but deviations as large as 100% were observed in the cases of malic and tartaric acid. By modifying the functional group parameters within the UNIFAC model, they improved the agreement of predictions and measurements to within 38% for the acids studied. As more experimental data become available, future improvements on the UNIFAC model should be expected.

[6] Here we report the deliquescence and efflorescence behavior of maleic acid mixed with ammonium sulfate. Maleic acid was chosen as a representative dicarboxylic acid based on its high solubility in water and presence in the atmosphere [Kawamura and Kaplan, 1987; Rohrl and Lammel, 2001; Saxena and Hildemann, 1996]. A temperature controlled flow tube system and Fourier Transform Infrared Spectroscopy (FTIR) were used to determine the deliquescence and efflorescence relative humidities of internally mixed maleic acid/ammonium sulfate particles for compositions ranging from 6 to 75 wt% maleic acid at 273 K. Water uptake by the particles prior to deliquescence was also observed and quantified.

2. Experiment

[7] A temperature-controlled flow tube system, shown schematically in Figure 1, was used to monitor the uptake and loss of water by the particles. This apparatus has been described in detail elsewhere [Onasch et al., 1999]. Briefly, aerosol particles are generated using an atomizer (TSI Model 3076) and a syringe pump (Harvard Apparatus 22) that supplies solution at a rate of $0.5 \text{ cm}^3/\text{min}$. The particle composition is set for each experiment by preparing and atomizing a solution of the desired wt% maleic acid. In this study, wt% maleic acid refers to the dry wt%, i.e. grams of maleic acid divided by total grams of maleic acid and ammonium sulfate, expressed as a percent. For all mixed

aerosol experiments, solutions were comprised of 170 grams of solute per 250 ml of water.

[8] For deliquescence experiments, aerosols generated by the atomizer are sent through a diffusion dryer and through a H_2SO_4 conditioner. In the conditioner, aerosol passes through the dry gas above a solution containing 95 wt% H_2SO_4 . Since the vapor pressure of H_2SO_4 in this conditioner is very low, $<10^{-4}$ Torr H_2SO_4 , we assume that no acid vapors interact with our aerosol sample. Upon leaving the conditioner, the RH is $<2\%$. The aerosol flow is then mixed with a dilution flow of humidified air from a temperature-controlled bubbler. Two 80 cm pretubes allow the aerosol to mix and equilibrate with its surrounding environment before reaching the 80 cm single pass FTIR observation tube. All flow tubes are double jacketed, allowing methanol/water coolant to circulate through the outer tubes. The coolant is controlled by a Neslab ULT-95 refrigerator, and temperature is monitored with five thermistors located within the aerosol stream and in the coolant flow of the observation tube and pretubes. During the deliquescence experiment, the relative humidity is incrementally increased by increasing the humidified flow from the bubbler, and FTIR spectra are taken at each point. Exiting the observation tube, a portion of the aerosol flow is continuously drawn through a heated Pallflex TA6060 filter and to an EdgeTech chilled mirror hygrometer at a rate of $500 \text{ cm}^3/\text{min}$. The remaining aerosol flow exits the system through an exhaust filter. The hygrometer measures the total water in the system. When no liquid water is present, the hygrometer provides a direct measurement of the relative humidity of the system. When condensed phase water is present in the aerosol, another technique must be employed to determine the gas phase water in the system. Specifically, gas phase water concentrations are measured during an experiment using FTIR spectroscopy. Prior to each aerosol experiment, the FTIR signal for gas phase water bands at $3658\text{--}3558 \text{ cm}^{-1}$ is calibrated to the RH, as determined from the hygrometer. A third-order polynomial fit is used to account for the apparent saturation of the IR peaks at high RH. During an aerosol experiment, the RH is determined by the calibrated IR signal from the gas phase

water bands. Once the total water measured by the hygrometer stabilizes, the FTIR spectra are recorded. Depending on the flow rate and relative humidity, the time for the system to adjust to the conditions is 1–10 min. The FTIR spectrometer also monitors condensed phase composition of the aerosol particles.

[9] For efflorescence experiments the bath in the H_2SO_4 conditioner contains a mixture of H_2SO_4 and water in proportions (~ 60 wt% H_2SO_4) chosen to ensure the aerosol enters the flow tube at 75–80% RH at 273 K. Deliquesced aerosol from the atomizer is sent through the H_2SO_4 conditioner and into the first pretube. The pretube has an additional inlet for a dry nitrogen dilution line to enter and mix with the aerosol at the temperature of interest. Throughout an efflorescence experiment, the relative humidity is decreased by incrementally increasing this dilution flow.

[10] All experiments in this study were performed at 273 K, the warmest controlled temperature setting on our Neslab cooling baths. Temperature gradients from the center of the observation tube to the coolant were ≤ 0.5 K causing an uncertainty in relative humidity of $\pm 2\%$. Our overall uncertainty for an individual experiment varies from ± 3 – 5% RH based on the temperature gradient, the precision of the hygrometer, and the increments in RH at which spectra were recorded throughout the experiment. We also conducted bulk measurements of the DRH at 273 K for mixed maleic acid/ammonium sulfate solutions. The bulk experimental method is described by Brooks *et al.* [2002]. Error in bulk RH measurements at 273 K are $\pm 3\%$ based on accuracy of the RH meter and slight temperature gradients measured in the gas phase. Error in composition is ± 2 wt%.

3. Aerosol Characterization

3.1. Infrared Spectroscopy

[11] Several methods were used to characterize the particles used in this study. The aerosol composition, i.e., the ratio of maleic acid to ammonium sulfate, is determined by the ratio of the two components in the solution atomized. Representative FTIR spectra of wet ammonium sulfate, wet 50 wt% maleic acid in ammonium sulfate, wet maleic acid ($\sim 95\%$ RH), and dry maleic acid ($\sim 2\%$ RH) are shown Figure 2a, Spectra I–IV, respectively. The gas phase water has been subtracted out of the each spectrum. The peaks used for analysis of aerosol composition are highlighted. In Spectrum II the mixed aerosol, we see the features of both pure ammonium sulfate (Spectrum I) and pure maleic acid (Spectrum III), indicating that both compounds have been successfully atomized. Furthermore, the ratios of the representative maleic acid peak heights to sulfate peak heights for solutions of varying ammonium sulfate/maleic acid content qualitatively reflect the composition of the initial solutions.

[12] For flow tube studies the liquid water content (LWC) of the aerosol is monitored as a function of RH using FTIR spectroscopy. LWC is defined as the integrated area of the liquid water peak at 3667 – 3358 cm^{-1} ratioed to the integrated area of a characteristic solute peak. Since the condensed phase water band at 3380 cm^{-1} is overlapping with the ammonium peaks at 3200 – 2800 cm^{-1} , we use only this narrow band for the integration of condensed phase water.

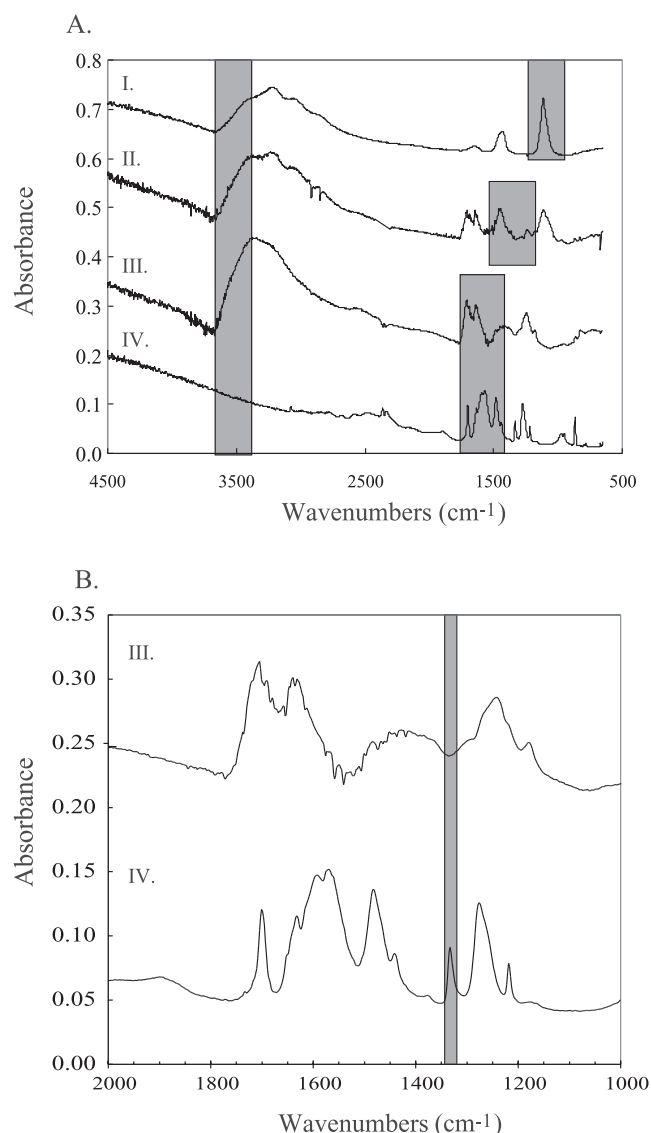


Figure 2. Representative FTIR spectra. (a) Wet ammonium sulfate, wet 50 wt% maleic acid/50 wt% ammonium sulfate, wet maleic acid, and dry maleic acid are shown in I, II, III, and IV, respectively. On the left, the integrated area of the liquid water peak is highlighted. On the right, the highlighted peaks indicate the aerosol peaks to which the integrated area of the liquid water is ratioed. (b) An expanded view of the FTIR spectra for wet and dry maleic acid in III and IV, respectively. The highlighted area in the spectra indicates the dry maleic acid peak.

[13] The purpose of ratioing to an aerosol solute peak is to normalize the liquid water signal to account for changes in dilution during an experiment. A different solute peak and baseline were chosen for each solute composition. In Figure 2a the liquid water and solute peaks used are highlighted at high and low wavenumbers, respectively. The solute peaks used in the analysis were chosen to avoid interference of neighboring peaks, and the baselines were chosen to optimize the signal to noise. The infrared regions used for integrations and baselines are indicated in Table 1.

Table 1. FTIR Integration

Composition	Integration Region, cm^{-1}	Baseline, cm^{-1}
Condensed phase water ^a	3653–3358	3667–2035
Ammonium sulfate ^b	1248–916	1248–916
Mixed		
Maleic acid/ammonium sulfate ^b	1572–1145	1778–1572
Maleic acid ^b	1766–1560	1766–1560
Dry maleic acid	1340–1328	1340–1328

^aUsed in all spectra.^bSolute band used for ratioing to determine LWC.

[14] In addition to the difference in LWC, other features differentiate the wet maleic acid spectrum from the dry. Figure 2b shows an expanded view of the FTIR spectra for wet and dry maleic acid in III and IV, respectively. It can be seen that dry maleic acid contains a sharp peak at $1340\text{--}1328\text{ cm}^{-1}$ that is not present in the solution spectrum. We do not think that this dry peak is an artifact, since it is observed only at low RH and there are accompanying changes at other wavelengths in the spectra at low RH. Moreover, aerosol particles are generated in the same way for all RHs throughout the experiments. To obtain low RH we simply add a dilution flow of prepurified nitrogen which is unlikely to contain significant impurities. Further, we note that this peak is not observed in other systems when we dilute with dry nitrogen to study efflorescence. To probe the identity of this peak observed in the maleic acid aerosol sample, we measured the infrared spectrum of a maleic acid thin film. The film was prepared by dissolving maleic acid in acetone and pipetting 2–3 drops onto a NaCl window. After evaporation of the solvent, the spectrum in Figure 3, Spectrum I, was observed. Shown for comparison in Figure 3, Spectrum II is a dry maleic acid aerosol spectrum taken in our flow tube at 10% relative humidity. As can be seen in the figure, the spectrum of the maleic acid film is similar to the dry maleic acid aerosol in most respects. However, the relative peak heights are slightly different, and the film spectrum does not contain the $\sim 1330\text{ cm}^{-1}$ peak identified in the dry aerosol spectrum. Since this peak is observed in the aerosol spectrum and not in the bulk, we surmise that it may be a surface feature. In addition, we compared these spectra to Sigma Aldrich's reference spectrum for condensed phase maleic acid (available at <http://www.sigma-aldrich.com>) (not shown). This reference spectrum looked very similar to the maleic acid film spectrum we measured.

[15] To ensure that the maleic acid in the particles was not being converted to its trans conformer (fumaric acid), during the flow tube experiments, we also prepared a thin film of fumaric acid. The spectrum obtained is shown in Figure 3, Spectrum III. As can be seen, the fumaric acid spectrum is quite different than the maleic acid spectrum, especially at wavenumbers higher than 1400 cm^{-1} . We conclude that the maleic acid aerosol is not being converted to fumaric acid during our flow tube experiments. The dry peak discussed above ($1328\text{--}1340\text{ cm}^{-1}$) is present in dry maleic acid aerosol spectra but not present in the dry maleic film spectra we took. Interestingly, a similar peak at these wavenumbers is present in the fumaric film spectra (Figure 3). *Maçoas et al.* [2001] performed calculations and made IR measurements of fumaric acid (trans) in an Argon isolation matrix.

They report that fumaric acid has three stable conformers which each have C-O stretches in our dry peak region. Based on this, we suggest that as maleic acid aerosol dries, most of it remains in the cis- isomer formation (i.e., maleic acid) but that at the surface some of the molecules may get bent to trans-like arrangements which gives rise to our dry peak. Alternatively, this dry feature could arise in the aerosol and not the bulk simply because the formation of different structures may be possible in particles.

[16] We also checked the possibility that our maleic acid particles were being converted to maleic anhydride at low relative humidity by comparing to the Sigma-Aldrich reference infrared spectrum for maleic anhydride (not shown). The maleic anhydride spectrum is, again, quite different than the dry maleic acid aerosol spectra we have observed, especially at $\sim 1350\text{--}1750\text{ cm}^{-1}$. We conclude that the aerosol is not being converted to maleic anhydride during the experiments.

[17] We thus believe that the 1330 cm^{-1} peak is most likely a surface feature present only on dry maleic acid particles. We note, however, that this peak is not readily discernable for dry mixed ammonium sulfate/maleic acid aerosols. This may be due to ammonium sulfate disrupting the surface environment for the feature or it may simply be due to overlap of the much larger sulfate stretch from ammonium sulfate.

3.2. Scanning Electron Microscopy

[18] In addition to FTIR spectroscopy, we used scanning electron microscopy (SEM) to determine whether

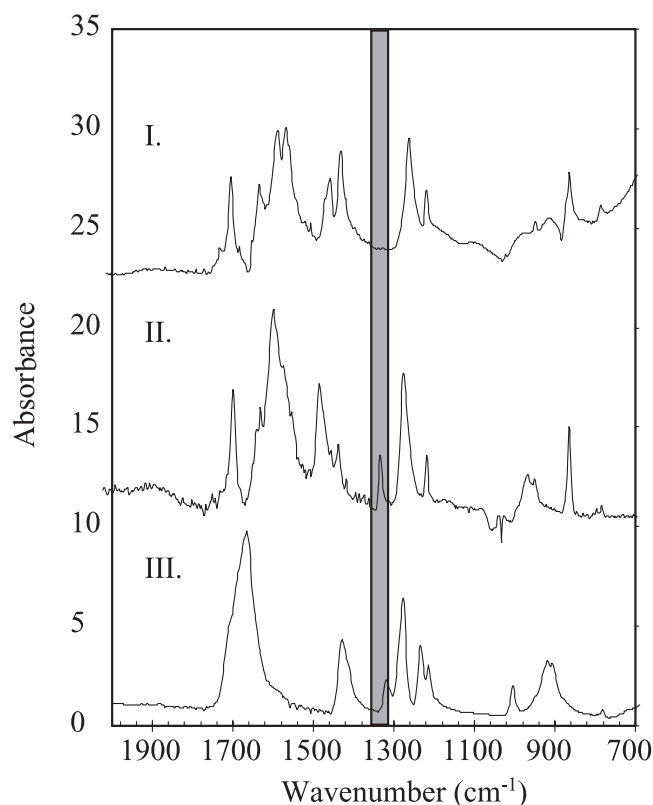


Figure 3. Infrared spectra of thin films and aerosol. Spectra of a maleic acid thin film, dry maleic acid aerosol, and a fumaric acid thin film are shown in 3I, 3II, and 3III, respectively.

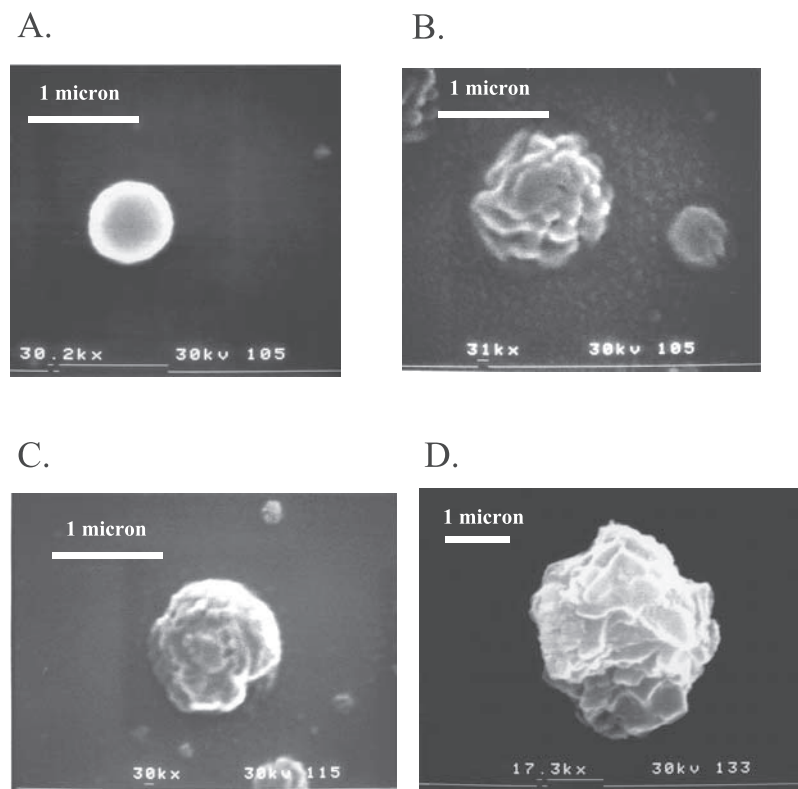


Figure 4. SEM images of ammonium sulfate, maleic acid, and 50 wt% maleic acid aerosol collected wet are shown in Figures 4a, 4b, and 4c, respectively. (d) The SEM image of 50 wt% maleic acid aerosol collected after the desiccant drying tube.

atomizing solutions containing both ammonium sulfate and maleic acid produced internally mixed particles or external mixtures of pure ammonium sulfate aerosol and pure maleic acid aerosol. The SEM images of ammonium sulfate, maleic acid, and 50 wt% maleic acid aerosols are shown in Figure 4. SEM samples were prepared by first atomizing a solution of the desired composition and collecting the wet aerosol sample on a gold plate for 1 min. In preparation for the scanning microscope, all samples were placed in a vacuum and plated with gold. Therefore all the images are of dry particles. The SEM images in Figure 4 are magnified to show the features of individual particles and are representative of the many SEM images of aerosols taken. It can be seen in Figure 4 that the pure ammonium sulfate particles are nearly spherical (Figure 4a), while the maleic acid particles have a more varied morphology (Figure 4b). The mixed aerosols also have a varied morphology (Figure 4c). No micrometer-sized spherical particles were observed in the mixed samples, suggesting that there were no pure ammonium sulfate particles when a 50 wt% maleic acid solution was atomized. For the mixed aerosol case, a second SEM sample was atomized and sent through a desiccant dryer and the dry aerosol was collected on the gold plate (Figure 4d). This was a test to determine if the desiccant dryer would cause phase separation. The particle in Figure 4d is very similar to the particle shown in Figure 4c. This shows that atomizing mixed solutions generates aerosols that remain internally mixed after

passing through the desiccant dryer and to the flow tube system.

3.3. Differential Mobility Analyzer and Condensation Particle Counter

[19] Finally, we used a differential mobility analyzer (DMA), TSI model 3080, and a condensation particle counter (CPC), TSI 3022A, to measure the size and number concentration of the aerosol samples used in this study. These studies were performed to check whether atomizing different solutions produces similar size distributions of particles. Since nucleation depends, in part, on particle size, we were interested in determining the sizes of our particles to check whether or not size could play a role in our study.

[20] To determine particle sizes, solutions were atomized, passed through a desiccant tube and sulfuric acid bath conditioner and sent to the DMA and CPC. The relative humidity throughout data collection, monitored using the dew point hygrometer, was $\sim 2.5\%$ or less, ensuring that the particles were dry. The DMA and CPC measurements were used to construct aerosol size distributions for ammonium sulfate, maleic acid, and 50 wt% maleic acid compositions.

[21] The average size and concentration parameters obtained for pure ammonium sulfate, pure maleic acid, and 50 wt% maleic acid are listed in Table 2. A lognormal fit to the ammonium sulfate data results in a count mean diameter, $d_C = 137$ nm and a standard deviation of $\sigma_c = 1.95$. Since the distribution is fairly wide, the surface area and volume mean diameters, 215 nm and 548 nm,

Table 2. Summary of Particle Statistics

Composition	Count Mean Diameter, nm	Standard Deviation	Concentration, #/cm ³	Surface Area Mean Diameter, nm	Volume Mean Diameter, nm
Ammonium sulfate	137	1.95	7.0×10^6	215	548
Maleic acid	154	2.03	6.9×10^6	253	585
50 wt% MA/AS	164	1.90	9.8×10^6	248	554

respectively, are significantly larger than the count mean diameter. The number concentrations measured by the CPC were roughly independent of composition. The volumes range from the largest size, 1.0×10^{-13} cm³ for a maleic acid particle, to 8.6×10^{-14} cm³ for an ammonium sulfate particle. Since the results show that the volumes of dry particles are similar, we conclude that the nucleation studies for all three cases can be directly compared.

4. Deliquescence of Maleic Acid/Ammonium Sulfate

4.1. Maleic Acid Deliquescence

[22] During a deliquescence experiment, we monitor the integrated area of the liquid water band at $3667\text{--}3358$ cm⁻¹, highlighted in Figure 2a, Spectra III and IV. In addition, we monitor the dry peak discussed above, $1328\text{--}1340$ cm⁻¹. For clarity, an expanded view of the FTIR spectra in the region of the dry peak at several relative humidities is shown in Figure 5. As can be seen in the figure as the RH changes, the spectra change in several ways. In particular, the dry peak is highlighted in the figure. This peak is not present in the spectra taken at higher relative humidity.

[23] The uptake of water by dry maleic acid particles as a function of RH is shown in Figure 6. In Figure 6a the liquid water band at $3667\text{--}3358$ cm⁻¹ is ratioed to a characteristic maleic acid stretch at $1766\text{--}1560$ cm⁻¹. It can be seen that maleic acid begins to take up water at a very low RH of $\sim 19\%$. Since we were concerned that the maleic acid peak chosen to normalize the liquid water content was changing

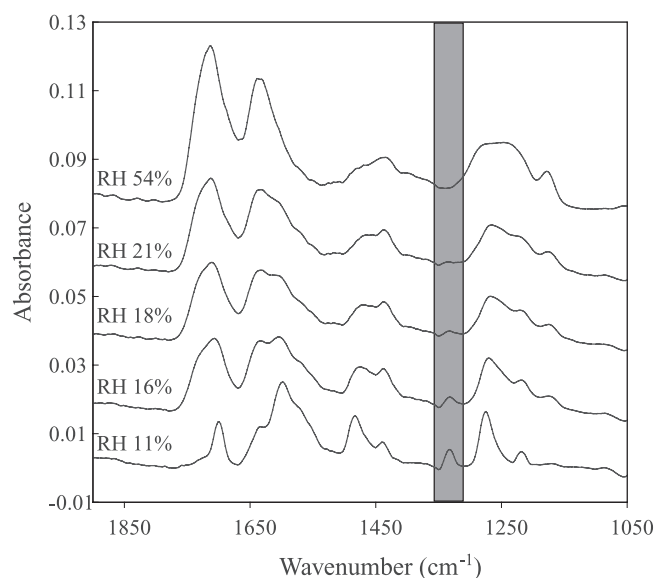


Figure 5. Infrared spectra of pure maleic acid aerosol as a function of relative humidity.

slightly as a function of relative humidity, we also plotted the integrated area of the uncorrected liquid water band, shown in Figure 6b. It can be seen that these two curves are in qualitative agreement with both showing water uptake at low RH with a sharp increase in water uptake near 90% RH. The sharp increase in water uptake at high RH is consistent with previous measurements of full deliquescence at 86–91% RH [Brooks *et al.*, 2002; Choi and Chan, 2002a]. However, Figure 6a suggests no water uptake below 19% RH, while Figure 6b could be interpreted as continual water uptake.

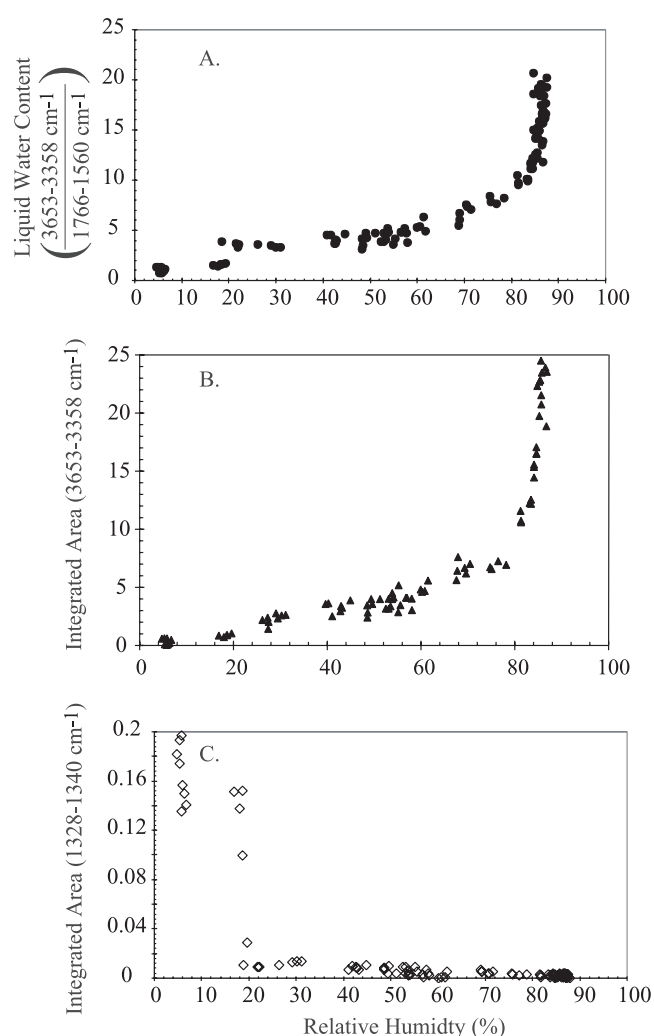


Figure 6. Liquid water content, the integrated area of condensed phase water, $3653\text{--}3358$ cm⁻¹, and the integrated area of the dry surface maleic acid peak, $1766\text{--}1560$ cm⁻¹, as a function of relative humidity are shown in Figures 6a, 6b, and 6c, respectively.

[24] To probe this further, we also integrated the area of the dry maleic acid aerosol peak discussed above, 1328–1340 cm^{-1} , as a function of RH (Figure 6c). Here it can be seen that there is a simultaneous increase in LWC (Figure 6a) and disappearance of the dry surface maleic acid peak at $\sim 20\%$ RH (Figure 6c). To quantify the amount of water taken up by the particles at 20% RH, we use a calibration of the FTIR signal.

[25] The calibration was performed at the deliquescence RH of 89% RH. At the DRH the ratio of water/maleic acid is known [Brooks *et al.*, 2002]. Our DMA and CPC study provides us with the dry particle size. Thus we can estimate the amount of water in the particles at the DRH and calibrate our FTIR condensed phase signal. Using this approach, we find that at the onset of water uptake the integrated area of the liquid water peak is $\sim 1\%$ of the maximum value of the integrated area we measured at the DRH.

[26] Because we may not have reached the true maximum value in our experiment, we assume $\leq 1\%$ of the moles required to deliquesce have been taken up at the RH of onset. Assuming we have a nonporous sphere of maleic acid, the observed liquid water at onset RH would be ≤ 88 monolayers. Because the morphology of a maleic acid particle is quite complex and nonspherical, at least when vacuum dried and gold-plated (Figure 4), the true surface area of the particles may be larger than that of a sphere. Thus the water coverage at 20% RH may be significantly less than 88 monolayers. However, this approximate calibration suggests that liquid water, in an amount on the order of monolayers, may be taken up by 20% RH.

[27] An alternative explanation for the water uptake is that a maleic acid hydrate has formed at 20% RH. However, there is no evidence in the IR for a hydrate, and in fact, the water band looks the same as the liquid water band. The water band at 20% RH is, however, quite small and we cannot rule out a small amount of hydrate formation at 20% RH.

[28] As the relative humidity is increased beyond 20%, the aerosol continues to take up additional water until its final deliquescence point of 89% RH. At the DRH there is a change to a continuous increase in LWC at a fixed relative humidity. In other words, at the DRH any additional water that is added to the system partitions to the particles. The RH remains constant until full deliquescence is completed. The observed DRH of 89% agrees within error with a study by Choi *et al.* [2002a] using a scanning electrodynamic balance to determine the DRH for water-soluble organic aerosols. They report the DRH for maleic acid as 86% RH. It also agrees fairly well with the bulk experiment described by Brooks *et al.* [2002] which reports a DRH of 91.9%. A significant difference between this aerosol flow tube study and the bulk study is the observation of water uptake prior to the DRH in the current work. Since bulk measurements can only be used to determine the DRH, water uptake prior to deliquescence would not be observable in a bulk study [Brooks *et al.*, 2002]. The assignment of the 1330 cm^{-1} peak as a dry surface feature is consistent with the observed behavior. If the surface adsorbed water, the surface properties would change well before the bulk properties. Thus our results are consistent with maleic acid adsorbing some surface water at $\sim 20\%$ RH followed by gradual uptake of water until the full DRH of 89%.

4.2. Deliquescence of Mixed Maleic Acid/Ammonium Sulfate Aerosols

[29] Maleic acid/ammonium sulfate aerosols were generated by atomizing a solution of the desired composition. To determine the LWC for mixed cases we measured the integrated area of the liquid water peak at 3667–3358 cm^{-1} ratioed to the integrated area of the ammonium peak in the ammonium sulfate at 1778–1560 cm^{-1} . Alternatively, we can calculate LWC by integrating the same liquid water peaks ratioed to the integrated area of the maleic acid peak at 1766–1560 cm^{-1} as in the maleic acid study. The DRH determined by both techniques was the same. For this study, we chose to use the sulfate peak since the signal to noise was slightly better.

[30] Figure 7 shows the deliquescence and onset results for 25, 50, and 75 wt% maleic acid. As can be seen in Figure 7a, the 50 wt% maleic acid has a significantly lower DRH than the 25 and 75 wt%. Figure 7b shows the results at low RH on an expanded scale to better show the onset of the water uptake. In all mixed cases containing ≥ 25 wt% maleic acid, water uptake begins at $\sim 20\%$ RH or less, similar to the pure maleic acid case. As indicated in the figure, the onset of water uptake occurs at approximately the same RH for all mixed compositions. The average RH of onset is $19\% \pm 3$. Within error, this is the same RH as the onset of water uptake by pure maleic acid aerosols.

[31] A summary of the onset of liquid water uptake (filled circles) and the full DRH (open circles) determined by the FTIR study are shown in Figure 8. The DRH for pure ammonium sulfate from a previous study conducted in our aerosol flow tube system, $\sim 81\%$ RH, is included for comparison [Onasch *et al.*, 1999]. Also shown in the figure are the DRH's determined by the bulk measurements of the DRH at 273 K, represented as filled triangles. For both the aerosol and the bulk, as the wt% maleic acid is increased, up to 50 wt%, the DRH becomes progressively lower. At compositions containing greater than 50 wt% maleic acid, there is an increase in the DRH. The bulk study predicts the DRH of pure maleic acid to be 91.9%. While the DRH values from the bulk study are slightly higher than the flow tube values, the two methods agree within error. The agreement between the aerosol and the bulk studies indicates that the deliquescence phase change is driven by the thermodynamic properties of the system. The bulk study predicts a DRH of 74.2 % RH for the eutonic composition, which has been determined to be ~ 45 wt% maleic acid [Brooks *et al.*, 2002]. This is consistent with the lowest measured the DRH in the flow tube study of 75% RH for the 50 wt% maleic acid case. As can be seen in Figure 8, the onset of water uptake prior to deliquescence was observed for compositions containing 25 wt% or more maleic acid. A small amount of water may have been taken up by aerosols containing less maleic acid in amounts below our detection limit.

5. Efflorescence of Maleic Acid/Ammonium Sulfate

5.1. Efflorescence of Maleic Acid

[32] Results from a representative efflorescence experiment for pure maleic acid are shown in Figure 9. The LWC and the integrated area of the dry surface maleic peak are shown in Figures 9a and 9b, respectively. Our results

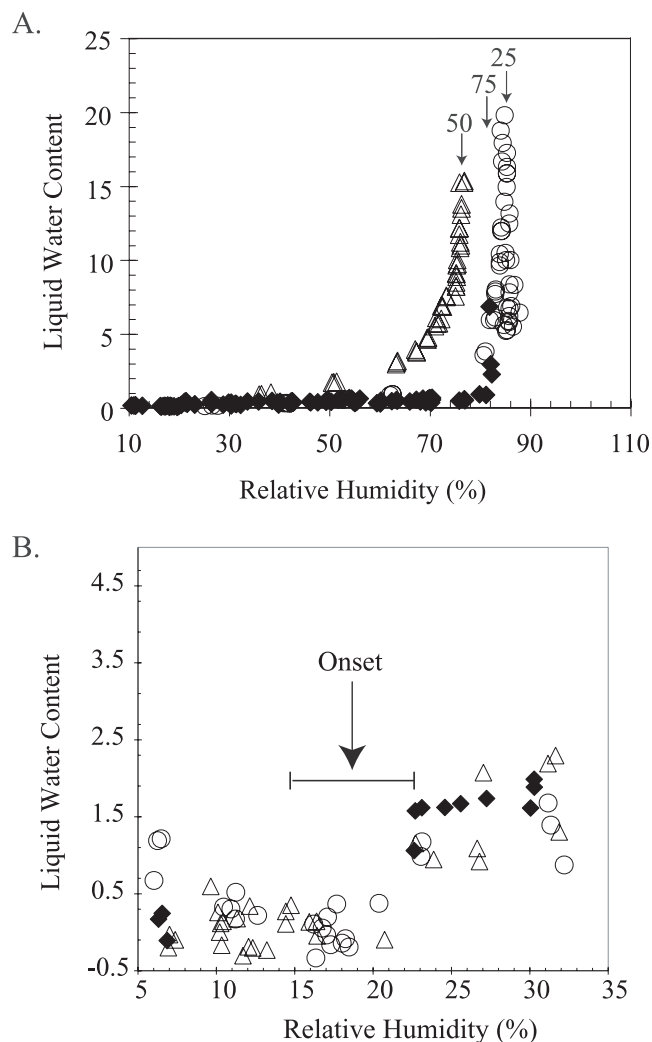


Figure 7. Deliquescence and onset of water uptake for mixed maleic acid/ammonium sulfate aerosols. The full range of RH and an expanded view of 10–35% RH are shown in Figures 7a and 7b, respectively. Results for 25, 50, and 75 wt% maleic acid are shown as open circles, open triangles, and filled diamonds, respectively. Dashed lines indicate DRH for each composition. In Figure 7B, the arrow and error bar indicate the average onset RH and the standard deviation for the onset RH of mixed aerosols of all compositions.

indicate that the efflorescence of maleic acid aerosols occurs at 17% RH at 273 K. This was determined by the highest RH at which LWC is below our signal to noise, ≤ 0.5 . Simultaneously at this RH, the dry surface maleic acid peak emerges in the infrared spectra. The disappearance of the dry peak during the deliquescence experiment and its reemergence during efflorescence occur at the same relative humidity, within our experimental error. However, the shape of the efflorescence curve shown in Figure 7a is very different than the deliquescence curve in Figure 6a. As the RH is reduced, the LWC is reduced slowly, indicating that the aerosol retains liquid water in a metastable state at RHs above the efflorescence RH. It is interesting to note that while our results indicate that a pure maleic acid

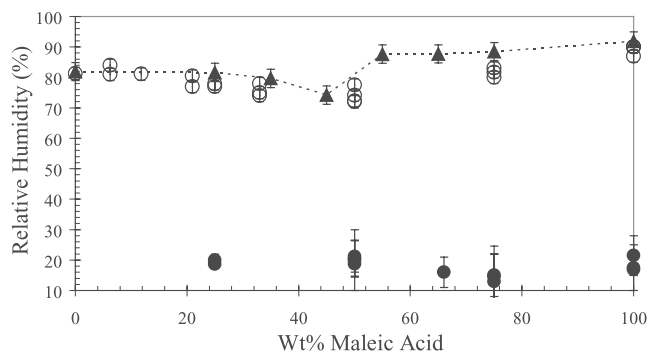


Figure 8. Summary of deliquescence as a function of RH at 273 K. Filled circles indicate the onset of water uptake in the FTIR experiments. Open circles and filled triangles indicate the DRH determined by FTIR experiments and bulk studies, respectively.

particle will not completely solvate until well above the DRH of ammonium sulfate, the efflorescence of pure maleic acid occurs at an RH significantly below 30% RH, the efflorescence point of pure ammonium sulfate.

5.2. Efflorescence of Mixed Maleic Acid/Ammonium Sulfate Aerosols

[33] We performed efflorescence experiments for mixed aerosols containing as little as 10 wt% maleic acid, and

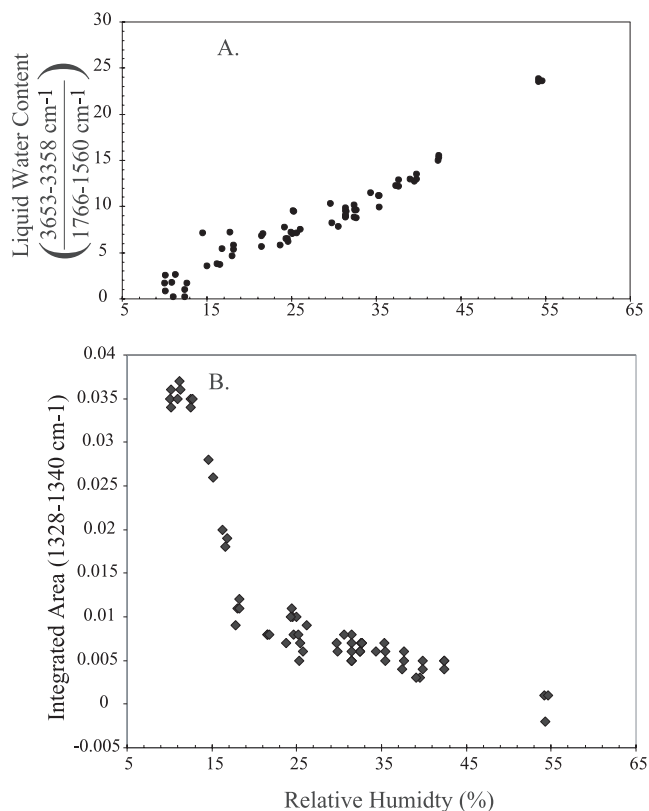


Figure 9. Efflorescence of pure maleic acid. The liquid water content and the integrated area of the dry surface maleic peak, 1766–1560 cm^{-1} , are shown in Figures 9a and 9b, respectively.

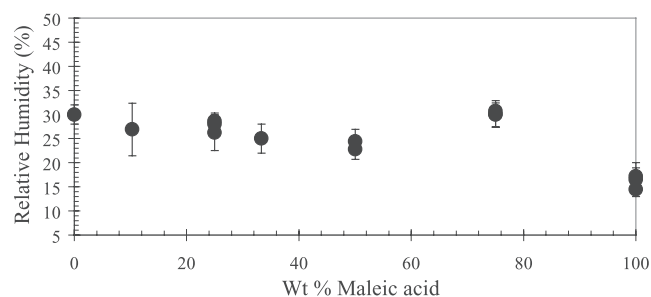


Figure 10. Summary of efflorescence relative humidity as a function of composition for mixed maleic acid/ammonium sulfate aerosol at 273 K.

our results are shown in Figure 10. It can be seen that the mixed aerosols effloresce at roughly the same RH, regardless of composition. The average efflorescence of aerosols of mixed composition occurs at $27 \pm 3\%$ RH, near the efflorescence point of the pure ammonium sulfate, 30% RH. Our results suggest that once the ammonium sulfate nucleates, it provides a heterogeneous nucleus, which induces the maleic acid to crystallize as well. In contrast, in the absence of heterogeneous nuclei, the pure maleic acid remains in solution until 17% RH. Similar observations have been reported by Choi and Chan [2002b] for succinic acid and glutaric acid mixed with ammonium sulfate. The less soluble component, in these cases the organic, crystallized first and formed nuclei for the salt. Of course, from our experiment we cannot determine which species initiated nucleation or if both species were involved.

6. Conclusions and Atmospheric Implications

[34] The results of our FTIR flow tube study show that mixed maleic acid/ammonium sulfate aerosol containing up to 50 wt% maleic acid exhibit full deliquescence at lower RH's than pure ammonium sulfate. Beyond a composition of 50 wt% the DRH of the mixed particles increases toward 91.9%, the DRH of pure maleic acid. In a complementary bulk study, we determined the DRH for a range of mixed aerosol compositions. The bulk measurements and flow tube aerosol results agree within error. In addition, for pure maleic acid and for mixed aerosols containing at least 25 wt% maleic acid, the onset of condensed phase water occurs at $\sim 20\%$ RH. The nature of this condensed phase is unclear but may be water adsorbed to the surface or may be caused by the formation of a maleic acid hydrate.

[35] The efflorescence of maleic acid was observed at $\sim 17\%$ RH. In contrast, the mixed aerosols effloresced at an average of $27 \pm 3\%$ RH regardless of the relative amounts of maleic acid and ammonium sulfate in the particles. Within error this is the same as the DRH of pure ammonium sulfate, $\sim 30\%$. This suggests that any ammonium sulfate present effloresces first and then acts as an efficient heterogeneous nucleus, inducing the efflorescence of the maleic acid. Therefore our results suggest that the presence of maleic acid in atmospheric aerosol would have little to

no effect on the efflorescence RH of ammonium sulfate aerosol.

[36] To the extent that maleic acid is representative of the water soluble organics present in atmospheric sulfate particles, our results suggest that under tropospheric conditions, the greater the water soluble organic content (up to 50 wt%) of an organic/ammonium sulfate aerosol, the more likely the aerosol is to be liquid. In contrast, a pure organic particle may deliquesce at a higher relative humidity than an ammonium sulfate particle. However, substantial amounts of liquid water may exist on pure organic particles prior to deliquescence, changing the chemical and physical properties of the particles.

[37] **Acknowledgments.** This work was supported by the Biological and Environmental Research Program (BER), U.S. Department of Energy, under grant DE-FG03-01ER63096. Matthew Wise was supported by a NASA Earth Science Fellowship, grant ESS/00-0000-0109. Melinda Cushing and Erika Hewitt were supported by the NSF-REU Program.

References

- Andrews, E., and S. M. Larson, Effect of surfactant layers on the size changes of aerosol particles as a function of relative humidity, *Environ. Sci. Technol.*, **27**, 857–865, 1993.
- Brooks, S. D., M. E. Wise, M. Cushing, and M. A. Tolbert, Deliquescence behavior of organic/ammonium sulfate aerosol, *Geophys. Res. Lett.*, **29**(19), 1917, doi:10.1029/2002GL014733, 2002.
- Choi, M. Y., and C. K. Chan, Continuous measurements of the water activity of aqueous droplets of water-soluble organic compounds, *J. Phys. Chem. A*, **106**, 4566–4572, 2002a.
- Choi, M. Y., and C. K. Chan, The effects of organic species on the hygroscopic behaviors of inorganic aerosols, *Environ. Sci. Technol.*, **36**, 2422–2428, 2002b.
- Clegg, S., J. Seinfeld, and P. Brimblecombe, Thermodynamic modeling of aqueous aerosols containing electrolytes and dissolved organic compounds, *J. Aerosol Sci.*, **32**, 713–738, 2001.
- Cruz, C. N., and S. N. Pandis, Deliquescence and hygroscopic growth of mixed inorganic-organic atmospheric aerosol, *Environ. Sci. Technol.*, **34**, 4313–4319, 2000.
- Ellison, G. B., A. F. Tuck, and V. Vaida, Atmospheric processing of organic aerosols, *J. Geophys. Res.*, **104**, 11,633–11,641, 1999.
- Hameri, K., and E. A. M. Rood, Hygroscopic properties of a NaCl aerosol coated with organic compounds, *J. Aerosol Sci.*, **23**, Suppl. 1, S437–S440, 1992.
- Hu, J. H., and J. P. D. Abbatt, Reaction probabilities for N_2O_5 hydrolysis on sulfuric acid and ammonium sulfate aerosols at room temperature, *J. Phys. Chem.*, **101**, 871–878, 1997.
- Kawamura, K., and I. R. Kaplan, Motor exhaust emissions as a primary source for dicarboxylic acids in Los Angeles ambient air, *Environ. Sci. Technol.*, **21**, 105–110, 1987.
- Krivacsy, Z., A. Hoffer, Z. Sarvari, D. Temesi, U. Baltensperger, S. Nyeki, E. Weingartner, S. Kleefeld, and S. Jennings, Role of organic and black carbon in the chemical composition of atmospheric aerosol at European background sites, *Atmos. Environ.*, **35**, 6231–6244, 2001.
- Loflund, M., A. Kasper-Giebl, B. Schuster, H. Giebl, R. Hitznerberger, and H. Paxbaum, Formic, acetic, oxalic, malonic and succinic acid concentrations and their contribution to organic carbon in cloud water, *Atmos. Environ.*, **36**, 1553–1558, 2002.
- Maçoas, E. M. S., S. R. Fausto, J. Lundell, M. Pettersson, L. Khriachtchev, and M. Rasanen, A matrix isolation spectroscopic and quantum chemical study of fumaric and maleic acid, *J. Phys. Chem. A*, **105**, 2922–3933, 2001.
- Mozurkewich, M., and J. G. Calvert, Reaction probability of N_2O_5 on aqueous aerosols, *J. Geophys. Res.*, **93**, 15,889–15,896, 1988.
- Murphy, D. M., D. S. Thomson, and M. J. Mahoney, In situ measurements of organics, meteoritic material, mercury, and other elements in aerosols at 5 and 19 kilometers, *Science*, **282**, 1664–1669, 1998.
- Onasch, T. B., R. L. Siefert, S. D. Brooks, A. J. Prenni, B. Murray, M. A. Wilson, and M. A. Tolbert, Infrared spectroscopic study of the deliquescence and efflorescence of ammonium sulfate aerosol as a function of temperature, *J. Geophys. Res.*, **104**, 21,317–21,326, 1999.
- Peng, C., M. N. Chan, and C. K. Chan, The hygroscopic properties of dicarboxylic and multifunctional acids: Measurements and UNIFAC predictions, *Environ. Sci. Technol.*, **35**, 4495–4501, 2001.

- Rohrl, A., and G. Lammel, Determination of malic acid and other C₄ dicarboxylic acids in atmospheric aerosol samples, *Chemosphere*, 46, 1195–1199, 2001.
- Saxena, P., and L. M. Hildemann, Water-soluble organics in atmospheric particles: A critical review of the literature and application of thermodynamics to identify candidate compounds, *J. Atmos. Chem.*, 24, 57–109, 1996.
- Tervahattu, H., K. Hartonen, V.-M. Kerminen, K. Kupiainen, P. Aarnio, T. Koskentalo, A. Tuck, and V. Vaida, New evidence of an organic layer on marine aerosols, *J. Geophys. Res.*, 107(D7), 4053, doi:10.1029/2000JD000282, 2002.
- Wexler, A., and J. H. Seinfeld, Second generation inorganic aerosol model, *Atmos. Environ.*, 25A, 2731–2748, 1991.

S. D. Brooks, M. Cushing, E. Hewitt, R. M. Garland, A. J. Prenni, M. A. Tolbert, and M. E. Wise, Department of Chemistry and Biochemistry and Cooperative Institute for Research in Environmental Sciences, University of Colorado, Boulder, CO 80309, USA. (sbrooks@lamar.colostate.edu; ehewitt@yahoo.com; garlandr@colorado.edu; prenni@lamar.colostate.edu; tolbert@spot.colorado.edu; Matthew.Wise@colorado.edu)